Improved image matching algorithm based on LK optical flow and grid motion statistics

Qunpo Liu* and Xiulei Xi

School of Electrical Engineering and Automation,
Henan Polytechnic University,
Jiaozuo, Henan, China
and
Henan International Joint Laboratory of
Direct Drive and Control of Intelligent Equipment,
Jiaozuo, Henan, China
Email: lqpny@hpu.edu.cn
Email: 2836963966@qq.com
*Corresponding author

Weicun Zhang

School of Automation,
University of Science and Technology Beijing,
Haidian, Beijing, China
Email: weicunzhang@263.net

Lingxiao Yang

School of Electrical Engineering and Automation,
Henan Polytechnic University,
Jiaozuo, Henan, China
Email: 1090452021@qq.com

Naohiko Hanajima

College of Information and Systems,
Muroran Institute of Technology,
Muroran, Hakkaido, Japan
and
Henan International Joint Laboratory of
Direct Drive and Control of Intelligent Equipment,
Jiaozuo, Henan, China
Email: hana@mondo.mech.muroran-it.ac.jp

Abstract: In order to solve the problems of low accuracy and long time-consuming of AKAZE algorithm in the image matching of glass encapsulated electrical connectors, an improved image matching algorithm based on LK optical flow and grid motion statistics is proposed. Matching points are obtained by calculating the matching area which are made up of the feature points for conditional constraints. In the local feature matching algorithm, large amount of calculation is an urgent problem as a result of sparse neighbourhood consistency feature cannot define adjacent areas well. The false matching points are removed by improved grid motion statistics algorithm based on integrates FLANN algorithm, and then match computation time is reduced. The performance is verified by experiments based on the Mikolajczyk and actual scene data. Experiment results show that the proposed algorithm can handle the actual scene data, the CMR reaches over 93%, and the time is within 0.4s.

Keywords: positioning; glass-encapsulated electrical connector; AKAZE algorithm; LK optical flow; feature matching; grid motion statistics.

Reference to this paper should be made as follows: Liu, Q., Xi, X., Zhang, W., Yang, L. and Hanajima, N. (2022) 'Improved image matching algorithm based on LK optical flow and grid motion statistics', *Int. J. Computer Applications in Technology*, Vol. 68, No. 1, pp.49–57.

Biographical notes: Qunpo Liu graduated from the Muroran Institute of Technology (Japan) with a PhD degree in Production Information Systems. He is an Associate Professor in the School of Electrical Engineering at Henan Polytechnic University (China) and a Master's Tutor. He is mainly engaged in teaching and research work in machine vision, robotics, intelligent control and industrial automation equipment.

Xiulei Xi graduated from the Luoyang Normal University. She is a Researcher in the Henan Polytechnic University (China). She is mainly engaged in machine vision.

Weicun Zhang is currently an Associate Professor in the School of Automation and Electrical Engineering, University of Science and Technology Beijing. He received his PhD degree in control theory from Tsinghua University in 1993. His research interests include self-tuning control, multiple model adaptive control and intelligent control.

Lingxiao Yang is a Professor in the School of Electrical Engineering at Henan Polytechnic University (China). She is mainly engaged in intelligent control and information processing.

Naohiko Hanajima graduated from the Hokkaido University (Japan) of Technology in Japan with a PhD. He is a Professor in the College of Information and Systems at Muroran Institute of Technology (Japan). He is mainly engaged in robotics and intelligent equipment.

1 Introduction

Stereo matching technology has become a key component of binocular vision positioning. It is widely used in the field of parts assembly. But there is a key problem to be solved that how to find the tested part and calculate its position quickly and accurately. Many computer vision tasks, such as motion recognition, motion tracking, robot navigation, and visual positioning rely on extracting local features from different views of the target image for achieving matching (Jinming et al., 2018). The glass-encapsulated electrical connector is a device which connects a precision component module and an internal circuit with a diameter of 0.6 mm. At present, it relies on manual assembly. In order to reduce costs, a method that binocular vision guides the robot is used to complete the assembly. The accuracy of the stereo matching of the two glass-encapsulated electrical connector images affects the positioning accuracy during the binocular vision positioning process seriously.

By now, the research on matching algorithms is mainly divided into two categories, one is to improve feature descriptors to improve performance, and the other is to increase constraints to eliminate mismatched points. In 2004, Lowe (2004) proposed the Scale-Invariant Feature Transform (SIFT) algorithm, which constructs a scale space through convolution of the original image and the Gaussian kernel, and then extracts the scale-invariant feature points from the Gaussian difference pyramid. The algorithm has affine, angle of view, rotation and illumination invariance, so it has been widely used in feature matching. Bay et al. (2006) proposed the Speeded-Up Robust Features (SURF) algorithm for the shortcomings of the slow speed and the amount of calculation in the calculation process of the SIFT algorithm. By using the approximate Harr wavelet algorithm for feature point extraction, the approximate Harr wavelet value is obtained by integration on different scale spaces, which reduces the construction of the second-order differential template, and improves the efficiency of feature matching. The Gaussian scale space constructed by these two methods is easy to ignore the edge detail information of the image. Alcantarilla et al. (2013) used nonlinear diffusion to describe features in a non-linear scale space, which preserves image edge information. A new 2D feature extraction method – Accelerated KAZE Features (AKAZE) descriptor is proposed. Shao et al. (2015) used the multi-resolution area detector MSER and the illumination robust shape descriptor to extract local areas from the input image for matching, and proposed a feature matching algorithm that is suitable for illumination changing images. Xing et al. (2016) proposed an algorithm for mismatching points for Oriented FAST and Rotated BRIEF (ORB) feature matching by reducing the total number of sampling points. In the same year, Lin et al. (2016) proposed a limit-guided feature matcher RepMatch for the poor object reconstruction effect, which can adapt to wide baselines and repeated structures, but the image of glass-encapsulated electrical connectors is not suitable for wide baselines. Tang and Peng (2017) solved the problem of logo recognition by using unique topological constraints to enhance the description ability of local features, but the topological constraints have not been extended to general objects. Bian et al. (2017) transformed the problem of motion smoothing restriction into statistical measurement to eliminate mismatches, and proposed an effective grid-based score estimator Grid-based Motion Statistics (GMS). But the GMS algorithm has a serious flaw, it doesn't have rotation invariance. Sedaghat and Mohammadi (2018) proposed an algorithm based on unified capabilities to solve the problem of local feature extraction of remote sensing images. This method used empirical parameters in the extraction process, which has certain limitations. In the same year, Prakash et al. (2019) used the combination of accelerated KAZE and scale-invariant feature transformation to propose a copy-movement forgery detection technology based on key points. Because the iterative solution obtained by the AKAZE algorithm using nonlinear equations is not unique, the current method still has the problem of feature point mismatching,

which results in a low image matching rate. Yan et al. (2020) used the FAST-SIFT algorithm to extract the characteristics of musculoskeletal images and solve the problem of musculoskeletal image stitching. The real-time and practicality of this algorithm need to be improved. In recent years, deep learning has continued to develop, and many researchers have applied neural networks to feature extraction. The method of this type requires a large amount of prior knowledge data (Dong et al., 2020; Wang et al., 2021). At present, the production conditions of glass-encapsulated electrical connectors are limited and the number of samples is not large, which results that this method is not applicable. Therefore, it is necessary to study traditional matching algorithms.

According to the above analysis, an improved image matching algorithm based on Lucas Kanade (LK) optical flow and mesh motion statistics is proposed to solve the problem of low image matching accuracy of glass package connectors. Based on the AKAZE feature detection algorithm, the LK optical flow and grid division statistics are combined to eliminate mismatched points and ensure the matching efficiency.

2 AKAZE feature target detection

The existing feature detection methods smooth the overall image of the glass-encapsulated electrical connector by constructing a Gaussian scale space, and it is easy to ignore the texture detail information of the glass-encapsulated electrical connector. In order to solve this problem, the AKAZE algorithm uses nonlinear filtering to construct a scale space to retain the edge information of the glass-encapsulated electrical connector, and perform local operations on the glass-encapsulated electrical connector. The principle of nonlinear filtering can be expressed as:

$$\partial L / \partial t = div\left(c\left(x,y,t\right)\cdot\nabla L\right) \tag{1}$$

where L represents the matrix of image brightness, *div* and ∇ represents the solution of divergence and gradient, respectively, t is the scale factor. The larger the value, the simpler the image performance, c represents the transmission function. The conduction spread function is defined as:

$$c\left(x,y,t\right) = g\left(\left|\nabla L_{\sigma}\left(x,y,t\right)\right|\right) \tag{2}$$

∇L_{σ} represents the gradient obtained after Gaussian smoothing of L, and the function g is:

$$g = \exp\left(-\frac{\left|\nabla L_{\sigma}\right|^2}{k^2}\right) \tag{3}$$

k is a contrast coefficient that controls the level of diffusion, and retains high-contrast edges preferentially. The nonlinear diffusion equation (1) is applied to the local structure of the image.

2.1 Construction of non-linear scale space

The scale space of the AKAZE algorithm is pyramid-shaped which has O groups and S layers. Through the spread function, the scale space is constructed according to time. The relationship between the scale parameter and the number of groups O and layers S is:

$$\sigma_i\left(O,S\right) = \sigma_0 2^{(o+s/S)} \tag{4}$$

The range of variables in formula (4) is: $o \in \left[0,1,...,O-1\right]$, $s \in \left[0,1,...,S-1\right], i \in \left[0,1,...,M-1\right]$. σ_0 indicates the initial scale parameter, which is the total number of images in the scale space, $M = O \times S$.

Since nonlinear diffusion filtering is related to time series, it is necessary to convert the scale parameter in pixels to time:

$$t_i = \frac{1}{2\sigma_i^2}, i = 0,1,\cdots,M \tag{5}$$

The Fast Explicit Diffusion (FED) algorithm is used to obtain the solution of equation (1). The nonlinear scale space of the image can be obtained as:

$$L^{i+1} = \left(I + \tau A\left(L^i\right)\right)L^i \tag{6}$$

In the formula, I is the identity matrix, $A\left(L^i\right)$ means that the image is passed to the matrix in dimension, τ is the step size and its value is $t_{i+1} - t_i$.

2.2 Feature detection

The comparison is preformed between a certain point with other points in its neighbourhood under different scale spaces. When the Hessian matrix achieves a maximum value, the key points can be located on the glass-encapsulated electrical connector. The calculation formula is:

$$L_{Hessian} = \sigma^2\left(L_{xx}L_{yy} - L_{xy}^2\right) \tag{7}$$

σ is the integer value of the scale factor σ_i. The exact position of the sub-pixel is found according to the Taylor expansion:

$$L(x) = L + x\left(\frac{\partial L}{\partial x}\right)^T + \frac{1}{2}xx^T\frac{\partial^2 L}{\partial x^2} \tag{8}$$

x is the position coordinates of the feature point, and the sub-pixel coordinates of the feature point are calculated as:

$$x = -\frac{\partial L}{\partial x}\left(x\frac{\partial^2 L}{\partial x^2}\right)^{-1} \tag{9}$$

2.3 Determine the main direction of feature points

The algorithm searches the gradient image with the feature point as the centre and the circle with the radius as the statistical range, and performs the Gaussian weighting operation on the first-order differential sum of all the inner neighbourhoods. Then it uses the fan-shaped area to rotate

around the origin to calculate the area vector sum. The main direction of the feature point is the longest direction in the vector sum.

2.4 Characteristic description

Binary descriptors are widely used in the process of target recognition and tracking because of their parallel computing and high efficiency. The AKAZE algorithm uses the Modified-Local Difference Binary (M-LDB) descriptor to sample the pixels and calculate the average value to achieve scale adaptation while ensuring real-time performance. Therefore, this descriptor is suitable for image matching of glass-encapsulated electrical connectors with higher matching requirements.

Figure 1 Schematic diagram of M-LDB descriptor

3 LK optical flow method matching area solution based on LK optical flow

LK optical flow method is widely used in the field of target tracking, and has some applications in feature point matching (Mao et al., 2019; Nigam and Tripathi, 2016). It is necessary to find the matching area and the characteristic point pair after detecting the key points of the glass-encapsulated electrical connector. And the LK optical flow method is introduced to track the characteristic points of the glass-encapsulated electrical connector to find the matching points.

On the assume that there are two greyscale images of glass-encapsulated electrical connectors I and J, he grey values at $[x, y]$ are respectively $I(x, y)$ and $J[x, y]$. There exists a pixel point $u = [u_x, u_y]$ on image I that matches pixel point $v = u + d = [u_x + d_x]^T$ on image J, so that the error between $I(u_x, u_y)$ and $J(u_x + d_x, u_y + d_y)$ is minimum. Displacement $d = [d_x, d_y]^T$ represents the optical flow of pixels u and v. In the range of the image $[2\omega_x + 1, 2\omega_y + 1]$ centred at the point u, the value of d is solved by finding the square sum of the minimum matching error. This loss function can be expressed as:

$$\varepsilon(d) = \sum_{x=u_x-\omega_x}^{u_x+\omega_x} \sum_{y=u_y-\omega_y}^{u_y+\omega_y} \left(I(x,y) - J\left(x + d_x, y + d_y\right)\right)^2 \quad (10)$$

The main process of the algorithm is to layer the image pyramid of the glass-encapsulated electrical connector, the lower layer is 1/2 of the upper layer, the top layer is the low-resolution image, and the bottom layer is the original image. The algorithm solves recursively from the top layer to the bottom layer in turn. Suppose the loss function of the L layer is:

$$\varepsilon(d) = \varepsilon^L = \sum_{x=u_x-\omega_x}^{u_x+\omega_x} \sum_{y=u_y-\omega_y}^{u_y+\omega_y} \left(I^L(x,y) - J^L\begin{pmatrix} x + g_x^L + d_x^L \\ , y + g_y^L + d_y^L \end{pmatrix}\right)^2 \quad (11)$$

In formula (11), g^L and d^L are respectively the initial value and error of the optical flow of the pixel point in the L layer iterative operation. According to Taylor's expansion, we can get:

$$\frac{1}{2}\left[\frac{\partial \varepsilon(\bar{v})}{\partial \bar{v}}\right]^T \approx \sum_{x=p_x-\omega_x}^{p_x+\omega_x} \sum_{y=p_y-\omega_y}^{p_y+\omega_y} \begin{bmatrix} I_x^2 & I_x I_y \\ I_x & I_y^2 \end{bmatrix} \bar{v} - \begin{bmatrix} \delta I I_x \\ \delta I I_{xy} \end{bmatrix} = G\bar{v} - \bar{b} \quad (12)$$

Then the optical flow extreme value $d_{opt} = G^{-1}b$, according to the optical flow d, the position on the image of the glass packaged electrical connector to be matched is determined, and then the matching area is solved.

4 Feature matching and removal of wrong matching points

The matching area is obtained by the mentioned LK optical flow method above, and feature matching is required in the next step. At present, the more commonly used algorithms are the BF algorithm and the Fast Library for Approximate Nearest Neighbours (FLANN) algorithm. The idea of the Brute Force (BF) algorithm is to calculate the distance between a certain feature descriptor and all other descriptors, sort the distance, and use the minimum distance to get the matching point. The FLANN algorithm is an open source library for nearest neighbours search, which optimises fast nearest neighbours search and high-dimensional features of large data sets. Since the BF algorithm only judges the matching points based on the distance between the descriptors, it is very easy to produce mismatching problems and the FLANN algorithm is introduced to solve the feature matching problem.

A is the part of the corresponding matching point set obtained after the initial matching of the image of the glass-encapsulated electrical connector, as shown in equation (9). There are many feature points in nearby correct matching points, so the mismatching can be eliminated based on this difference. After the initial matching of the image of the glass-encapsulated electrical connector, A is the part of the corresponding matching point set obtained

$$A_{i,L-R} = \{a_1, a_2, ..., a_n\} \quad (13)$$

The distribution of matching points can be expressed as:

$$S(a_i)=\begin{cases} B(Kn,p_1),a_i \text{ is the correct match} \\ B(Kn,p_2),a_i \text{ is the incorrect match} \end{cases} \tag{14}$$

The equation (14) represents the matching point pair between the matched area and the area to be matched, K represents the number near the small area, n is the number of matching pairs, p_1 and p_2 are the correct and incorrect matching rates, respectively.

The algorithm determines whether to exclude matching points according to the value of the probability evaluation standard function.

$$p_a=\frac{\sqrt{Kn}(p_1-p_2)}{\sqrt{(1-p_1)+(1-p_2)}} \tag{15}$$

It can be seen from formula (13) that p_a is proportional to $\sqrt{Kn}$, indicating that the more image feature points are extracted, the larger the value p_a obtained, the higher the matching accuracy.

5 Improved image matching algorithm

Since the use of AKAZE feature extraction to solve partial differential equations will produce multiple sets of solutions, there may be mismatch problem. Improved image matching algorithm based on LK optical flow and grid motion statistics is proposed to solve this problem. The algorithm includes the following steps:

1) Feature extraction and description of AKAZE feature points are performed on the original glass package electrical connector image. And matching them with the feature points of the image to be matched.
2) An image pyramid is constructed after feature description of two glass-encapsulated electrical connector images, and the optical flow is solved by using equation (12) in the LK algorithm to obtain the matching area, and the feature points are tracked.
3) Feature matching is required after detecting and describing feature points. The FLANN algorithm library is introduced to realise this function.
4) After the FLANN feature matching, there are some mismatching points in the glass-encapsulated electrical connector image. At this time, the glass-encapsulated electrical connector image is divided into multiple grids and the number of matching points in nearby feature points is calculated. According to equation (11), the probability value can be derived. The larger the value is, the higher the probability of correct matching is.

Figure 2 Matching algorithm flow chart

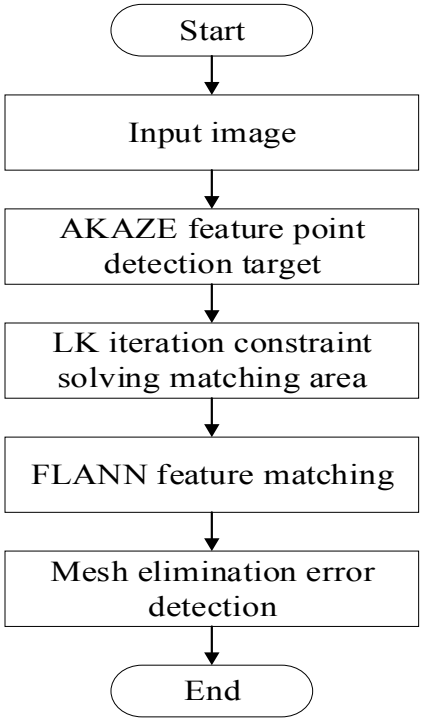

6 Experimental results and analysis

In order to test the matching ability of the algorithm, the public data set Mikolajczyk (Yang et al., 2014) and the actual scene glass package electrical connector image are used for simulation experiment, and the algorithm in this paper is compared with the SIFT algorithm, SURF algorithm and AKAZE algorithm. The algorithm is evaluated in two aspects including the matching effect and algorithm consumption. The experiments are performed based on a PC with Intel i5 CPU, 1.60–1.80, 8 GB memory and 64-bit Windows10 operating system. The algorithm experiment in this paper is based on OenCV3.4.2, the programming language is Python, and the programming environment is Pycharm2017. The experiment consists of four parts: fuzzy image matching experiment; brightness variation matching experiment; rotation variation matching experiment; glass package electrical connector image matching experiment. The Figure 3 shows bike image pair, Leuven image pair, boat image pair and glass package electrical connector image pair.

6.1 Fuzzy image matching experiment

In order to verify the matching performance of the algorithm in this paper for fuzzy images, the Bike image are used. The fuzzy matching result is shown in Figure 3. Other algorithms are more sensitive to fuzzy image matching by analysing the data in Figure 4.

Figure 3 Image pair to be matched. (a) bike image pair (b) luaven image pair (c) boat image pair (d) glass package electrical connector image pair

(a)

(b)

(c)

(d)

Figure 4 Experimental results of fuzzy image matching. (a) SIFT algorithm (b) SURF algorithm (c) AKAZE algorithm (d) Proposed algorithm

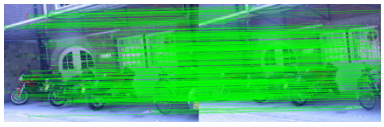

(a)

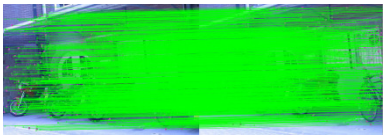

(b)

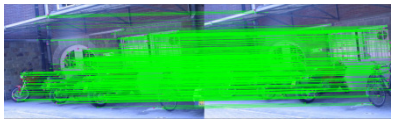

(c)

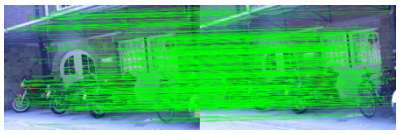

(d)

6.2 *Image matching experiment with different bright image*

In the matching process of actual applications, it is a common phenomenon that there are some brightness changes. In order to test the matching performance of the algorithm to different brightness images, the Leuven image are used to achieve different brightness matching effects as shown in Figure 5.

Figure 5 Experimental results with different bright image. (a) SIFT algorithm (b) SURF algorithm (c)AKAZE algorithm (d) Proposed algorithm

(a)

(b)

(c)

(d)

6.3 *Rotation variation matching experiment*

In order to verify that the algorithm in this paper has rotation invariance to the image, (using Boat image) the algorithm in this paper is compared with the SIFT algorithm, the SURF algorithm and the AKAZE algorithm. According to the experimental results, the algorithm proposed in this paper can achieve the best accuracy.

6.4 *Image matching experiment with glass-encapsulated electrical connector*

Figure 7 shows the matching results of each algorithm. It can be seen that the proposed algorithm has a higher rate of feature matching, and other algorithms match the wrong information when there is interference in the background.

Figure 6 Experiment results of rotation image. (a) SIFT algorithm (b) SURF algorithm (c)AKAZE algorithm (d) Proposed algorithm

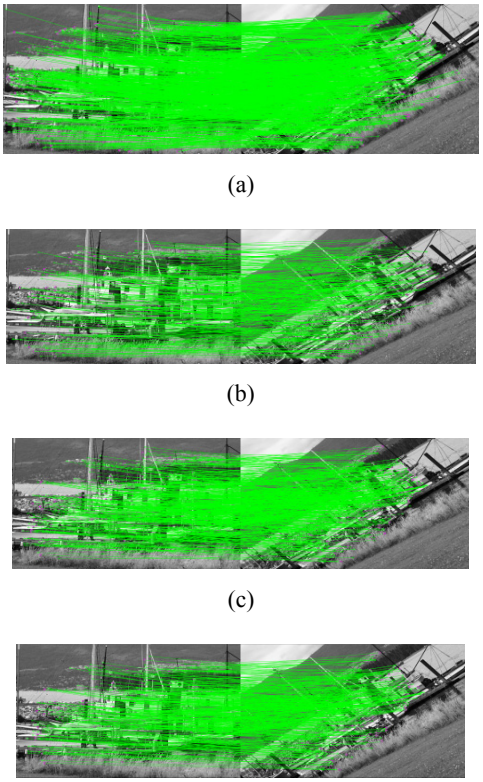

(a)

(b)

(c)

(d)

6.5 Comparison of matching performance

The matching performance is mainly measured by the matching accuracy and time of two indicators. CMR stands for matching accuracy, which means the percentage of the number of pairs of correct points to the number of pairs of matching points. The larger the value is, the higher the matching accuracy is. The matching accuracy results of this algorithm, SIFT algorithm, SURF algorithm and AKAZE are shown in Figure 8. Through the analysis of the number of matching points and the correct rate of the public data set and the image of the glass package electrical connector in the figure below, it can be seen that the number of matching points detected by the SIFT algorithm is the largest, but the correct rate is also low. Although the number of matching pairs obtained by the algorithm in this paper is slightly smaller, comparing with other algorithms, its accuracy can be improved effectively.

Comparing the time consumption of the algorithm in this paper with the SIFT, SURF, and AKAZE algorithms. Figure 9 and Table 1 show the time-consuming results of the four algorithms. The LK optical flow algorithm greatly reduces the number of matching points and ensures the accuracy of the matching by increasing the constraint conditions.

Figure 7 Experimental results of glass-encapsulated electrical connector. (a) SIFT algorithm (b) SURF algorithm (c)AKAZE algorithm (d) Proposed algorithm

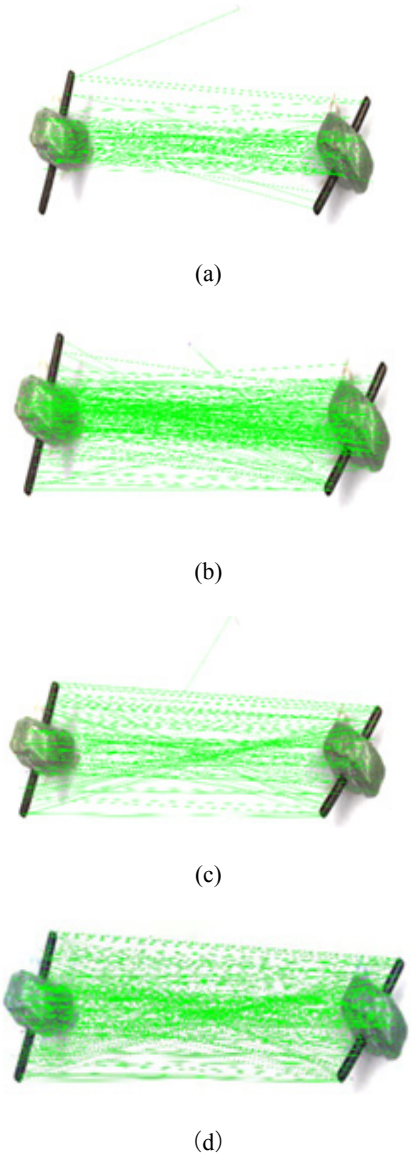

(a)

(b)

(c)

(d)

Figure 8 Comparison of matching CMR

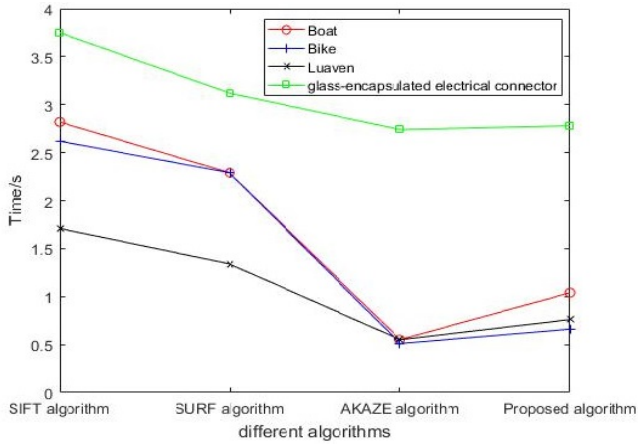

Figure 9 Comparison of time consumption

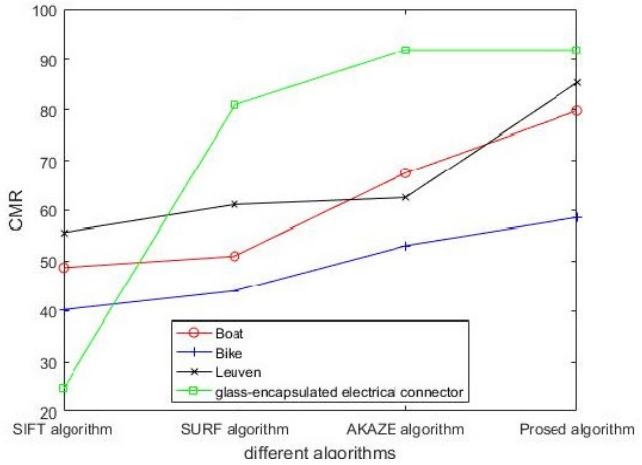

Table 1 Comparison of image matching accuracy and time of image pair

Image change	*Algorithm*	*Number of matching points*	*Correct point logarithm*	*CMR (%)*
Rotation change	SIFT	2674	1303	48.72
	SURF	800	408	50.99
	AKAZE	735	496	67.49
	This paper	735	3563	79.83
Lighting change	SIFT	1638	659	40.22
	SURF	3708	1631	43.99
	AKAZE	1576	825	53.10
	This paper	1576	924	58.62
Blur change	SIFT	205	114	55.68
	SURF	2849	1743	61.17
	AKAZE	1499	624	62.54
	This paper	1499	1755	85.41
Actual scene image pair	SIFT	759	187	24.65
	SURF	300	243	81.00
	AKAZE	138	127	92.03
	This paper	138	128	93.03

7 Conclusions

In order to solve the problem of mismatch and time-consuming in the image matching process of glass package connectors, an improved image matching algorithm based on LK optical flow and grid motion statistics is proposed, and the problem of lots of mismatches is solved by adding constraints. Based on the AKAZE feature detection method, an image pyramid is constructed as the control point of the LK optical flow. The matching area is calculated, and the feature points are used for grid division to reduce false matching after the FLANN matching. The results show that the algorithm proposed in this paper can effectively improve the matching accuracy even in the case of rotation, illumination and blur, when applied to the image of the glass package connector. In future work, feature descriptors can be studied to further reduce the time consumed by the algorithm.

Acknowledgements

This work is partially supported by the National Key Research and Development Program (No. 2016YFC0600906); Science and Technology Innovation Team of Colleges and Universities in Henan Province (No. 20IRTSTHN019); Innovative Science and Technology Talents Team Construction Project of Henan Province (No. CXTD2016054); Science and Technology Project of Henan Province (No. 212102210508).

References

Alcantarilla, P.F. et al. (2013) 'Fast explicit diffusion for accelerated features in nonlinear scale spaces', *British Machine Vision Conference*, pp.1–12.

Bay, H., Tuytelaars, T. and Gool, L.V. et al. (2006) 'SURF: speeded up robust features', *European Conference on Computer Vision*, pp.7–13.

Bian, J., Lin, W.Y. and Matsushita, Y. et al. (2017) 'GMS: grid-based motion statistics for fast, ultra-robust feature correspondence', *Computer Vision and Pattern Recognition*, pp.4181–4190.

Dong, Z., Li, G. and Liao, Y. et al. (2020) 'CentripetalNet: pursuing high-quality keypoint pairs for object detection', *IEEE/CVF Conference on Computer Vision and Pattern Recognition*, Doi: 10.1109/CVPR42600.2020.01053.

Jinming, Z., Zuren, F. and Jinpeng, Z. et al. (2018) 'An improved randomized local binary features for keypoints recognition', *Sensors*, Vol. 18, No. 6, pp.1937–1961.

Lin, W.Y., Liu, S. and Jiang, N. et al. (2016) 'RepMatch: robust feature matching and pose for reconstructing modern cities', *European Conference on Computer Vision*, pp.562–579.

Lowe, G. (2004) 'SIFT-The scale invariant feature transform', *International Journal (Toronto, Ont.)*, Vol. 2, pp.91–110.

Mao, L., Pu, Y. and Wang, L. (2019) 'Research on robot location based on an improved method of map feature matching', *Neurocomputing*, Vol. 6, No. 4, pp.332–338.

Nigam, A. and Tripathi, R.C. (2016) 'Trademark image retrieval using weighted combination of sift and HSV correlogram', *Neurocomputing*, Vol. 54, No. 1, pp.61–67.

Prakash, C.S., Panzade, P.P. and Om, H. et al. (2019) 'Detection of copy-move forgery using AKAZE and SIFT keypoint extraction', *Multimedia Tools and Applications*, Vol. 7, pp.23535–23558.

Sedaghat, A. and Mohammadi, N. (2018) 'Uniform competency-based local feature extraction for remote sensing images', *Isprs Journal of Photogrammetry and Remote Sensing*, Vol. 135, pp.142–157.

Shao, Z., Chen, M. and Liu, C. (2015) 'Feature matching for illumination variation images', *Journal of Electronic Imaging*, Vol. 24, No. 3, pp.033011.1–033011.11.

Tang, P. and Peng, Y. (2017) 'Exploiting distinctive topological constraint of local feature matching for logo image recognition', *Neurocomputing*, Vol. 5, No. 236, pp.113–122.

Wang, H., Pan, T. and Ahsan, M.K. (2021) 'Hand-drawn electronic component recognition using deep learning algorithm', *International Journal of Computer Applications in Technology*, Vol. 62, No. 1, pp.13–62.

Xing, K., Ling, Y. and Chen, M.Y. (2016) 'Mismatching points elimination algorithm for ORB feature matching', *Journal of Electronic Measurement and Instrumentation*, Vol. 30, No. 8, pp.1255–1262.

Yan, H., Zhang, P. and Wang, Y. et al. (2020) 'Feature detection algorithm of musculoskeletal ultrasound image and its application of image stitching', *Journal of Image and Graphics*, Vol. 25, No. 5, pp.1032–1042.

Yang, X., Huang, C. and (Tim) Cheng, K.T. (2014) 'LDB: a library for extracting ultrafast and distinctive binary feature description', *ACM International Conference*, pp.671–674.